Journal of Statistical Physics, Vol. 69, Nos. 1/2, 1992

Fluctuation Effects in Models of Adiabatic Explosion

Dong-Pao Chou,[1] Thomas Lackner,[2,3] and Sidney Yip[2]

Received December 20, 1991; final March 27, 1992

Models of thermal explosion in a closed system are studied at the macroscopic level, where a nonlinear rate equation is solved numerically, at the stochastic level, where the corresponding master equation is solved numerically and also analyzed through a $1/N$ expansion (N is the number of particles in the system) and at the atomistic level, where molecular dynamics simulations of reacting hard disks are carried out. We find that for 800 particles ($N = 800$) simulation gives sufficient agreement with the macroscopic description of the average concentration. In the region of $N = 50$–2000 the stochastic and molecular dynamics results show significant overlap with each other; as expected, the effects of fluctuations decrease with increasing N. Under a low-temperature condition (slow reaction rate), a regime which cannot be realized in molecular dynamics simulation, direct numerical solution of the master equation reveals a bimodal distribution during times comparable to a correlation time. This behavior of transient bifurcation, which had been discussed previously, is shown to be a result of small system size.

KEY WORDS: Adiabatic explosion models; nonlinear fluctuations; master equation and $1/N$ expansion; molecular dynamics simulation.

1. INTRODUCTION

It is well known that a system of reacting particles can exhibit rapid transient behavior as a consequence of strong nonlinearities inherent in the reaction kinetics. Such transients are traditionally studied by means of continuum rate equations with or without spatial effects. However, in a more fundamental approach to the understanding of reactive systems it

[1] Institute of Nuclear Energy Research, Atomic Energy Council, Lung-tan, Taiwan, Republic of China.

[2] Department of Nuclear Engineering, Massachusetts Institute of Technology, Cambridge, Massachusetts 02139.

[3] Present address: Siemens AG, Munich 83, Germany.

0022-4715/92/1000-0193$06.50/0

would be necessary to consider the effects of fluctuations as the systems are driven far from equilibrium (see, e.g., refs. 1). For thermal fluctuations in nonlinear chemical systems, analysis of a model of adiabatic explosion[2] has shown, among other features, the existence of a multipeak concentration distribution of reactants, a behavior which has been called "time bifurcation" or "internal time differential,"[3] and "transient bimodality."[4] Since this behavior clearly arises from fluctuations, further investigations of the nature of such fluctuations seem worthwhile.

In this work we present a study of adiabatic explosion at three complementary levels, a macroscopic level based on a nonlinear rate equation, a stochastic level involving a master equation with a certain transition rate, and the atomistic level of molecular dynamics simulation. Since fluctuations are absent in the macroscopic equation, this level of analysis provides the reference results for the delineation of fluctuation effects treated at the other two levels. By combining the stochastic description with dsiscrete-particle simulation, we obtain a test of the master equation formulation and solution, as well as an extension of the simulation study to larger system sizes (number of particles). To our knowledge, such an integrated approach has not been reported previously.

In adiabatic explosion (explosion in a closed vessel[5]) all the energy released from a reaction is converted into raising the system temperature. This property enables the reactant concentration to be directly related to the system temperature, thus simplifying the analysis significantly. At the macroscopic level one has a rate equation of the Arrhenius form, and the time-dependent reactant concentration therefore can be determined by quadrature. In formulating the corresponding master equation description, one has a system of coupled equations governing the probability distribution function, with Arrhenius kinetics expressed through an appropriate transition probability. For pure death processes as is the present case, the equations can be given a series solution[3] which, in practice, becomes difficult to compute for a large number of particles. In the case of molecular dynamics simulation there is also a restriction on the number of particles that can be studied, although the reason here is one of computational burden in contrast to the problem of convergence in the above series solution. Although the connection between the different methods of description may be intuitively clear, the objective of this study is to work out the results in detail to investigate the complementarity between these methods.

In Section 2 we define the basic adiabatic explosion model and consider two slightly different versions, one corresponding to unimolecular reactions[2,3] and the other to collision-induced reactions. In Section 3 we begin with the master equation for pure death processes and express it as an equation for a conditional average. The latter is then solved in a $1/N$

expansion, where N is the number of particles in the system. This solution is useful for examining the effects of fluctuations since in the limit of large N all fluctuation effects vanish and one recovers the solution to the macroscopic rate equation. In Section 4 we briefly describe the molecular dynamics model of two-dimensional hard disks used to simulate adiabatic explosion. The results of all three levels of analysis are presented and discussed in Section 5. The broader implications of these results are discussed in the concluding remarks given in Section 6.

2. ADIABATIC EXPLOSION MODELS

In modeling rapid exothermic reactions in a closed system[2,3] we imagine reactant particles A undergoing reactions at a rate k which has a temperature dependence of the Arrhenius form. Product particles B formed are inert, and since no energy can be transferred to the surroundings, all the heat of reaction goes into raising the system temperature. In the case of unimolecular reaction[2,3]

$$A \xrightarrow{k[T]} B \tag{2.1}$$

One can also consider a bimolecular reaction

$$A + A \xrightarrow{k'[T]} A + B \tag{2.2}$$

which would be appropriate to collision-induced processes in gas phases. The reaction rates $k[T]$ and $k'[T]$ will have somewhat different concentration dependence (and therefore different temperature dependence); on the other hand, the fluctuation behavior of the two models should not differ qualitatively.

In terms of a macroscopic description the problem is to study the time dependence of the reactant concentration. If we let $\bar{n}_A(t)$ denote the average number of particles A at time t, and N the total number of particles in the system, then the concentration $\bar{x}(t) = \bar{n}_A(t)/N$ satisfies

$$\frac{d\bar{x}(t)}{dt} = -\mu(\bar{x}) \tag{2.3}$$

with reaction rate $\mu(\bar{x})$ depending on the model adopted. For the unimolecular reaction, (2.1), which we wil call model a, one has

$$\mu_a = \alpha n_A e^{-U/T} \tag{2.4}$$

where α is a proportionality constant, U is the activation energy, and T is the temperature (in units of Boltzmann's constant). For the collision-induced reaction, (2.2), model b,

$$\mu_b = \alpha' n_A z_{AA} e^{-U/T} \tag{2.5}$$

where α' is another constant and z_{AA} is the collision frequency. Using the expression for hard spheres in the limit of low velocity, $v \ll v_T$, where $v_T = (2T/m_A)^{1/2}$ is the thermal velocity, with m_A being the particle mass, one finds $z_{AA} = 2\sqrt{\pi}\, n_A \sigma_{AA}^2 v_T$.

Since we restrict our considerations to a pure death process only, $\mu(\bar{x}) > 0$, so the concentration must decrease monotonically with time until all reactants are exhausted. As the system evolves toward this final state, it will pass through a transient period when $\mu(\bar{x})$ is near its maximum. During this period, which we may characterize as ignition or explosion, the system appears to be most chaotic and fluctuations effects are most pronounced.[2-4]

The macroscopic equation (2.3) gives no information about fluctuations. For a stochastic description one can introduce a master equation,

$$\frac{dP(n, t \mid n_0)}{dt} = \mu(n+1)\, P(n+1, t \mid n_0) - \mu(n)\, P(n, t \mid n_0) \tag{2.6}$$

where $P(n, t \mid n_0)$ is the probability of having n number of A particles at time t given that at $t = 0$ there were n_0 particles of this species. The initial condition is $P(n, 0 \mid n_0) = \delta_{n,n_0}$; also, in order that (2.6) holds for $n = 0$ to n_0, one needs to specify $\mu(n_0 + 1) = \mu(0) = 0$.

Both the macroscopic and the stochastic descriptions are specified once the reaction rate $\mu(\bar{x})$ or $\mu(n)$ is known. For the two models above we can write

$$\mu_a(n) = \alpha n \exp[-U/(T_m - r_v n/C_v N)] \tag{2.7}$$

$$\mu_b(n) = \alpha'' n^2 \sqrt{T} \exp[-U/(T_m - r_v n/C_v N)] \tag{2.8}$$

where α'' is a constant, T_m is the maximum temperature (system temperature in its final state), r_v is the heat of reaction, and C_v is the specific heat. In rearranging the Arrhenius factor, we have used the adiabatic condition

$$C_v T + r_v n/N = C_v T_m \tag{2.9}$$

Neither model a nor model b is tractable from the standpoint of analytical study. As a simplified nonlinear model which is amenable to analysis, we will consider the quadratic approximation (model c)

$$\mu_c(n) = \gamma n(1 - n/N) \tag{2.10}$$

where γ is a constant. This quadratic approximation is a special form of the more general Malthus–Verhulst equation which includes both a birth and a death rate. Notice that $\mu_c(n)$ follows from $\mu_a(n)$ if $T \gg U$ and $r_v n_0 \gg T_0$, where T_0 is the initial system temperature $T_0 = T_m - r_v n_0 / C_v N$. We will find that the behavior of this model is useful for understanding the nature of the double hump in the probability distribution function. This model has been used in the literature in population studies.[6]

Models *a* and *b* involve three parameters, which can be chosen to be the initial concentration $x_0 = n_0/N$ and dimensionless initial and final temperatures $\theta_0 = T_0/U$ and $\theta_m = T_m/U$. In contrast, model *c* involves only the parameter γ. In this model one cannot choose the initial concentration to be $x_0 = 1$, since that would make μ_c identically zero and the system would never react. In practice any value $x_0 < 1$ would not give rise to this difficulty.

3. THE 1/*N* EXPANSION

In order to analyze the stochastic behavior of the adiabatic explosion models, we will introduce a method of treating the master equation for pure death processes. We begin with the backward form of the master equation[7–10]

$$\frac{dP(n, t \mid n_0)}{dt} = \mu(n_0)[P(n, t \mid n_0 - 1) - P(n, t \mid n_0)] \tag{3.1}$$

One can show that this description is equivalent to the forward form of the master equation (2.6). Baras *et al.* have given a series solution to (2.6) with the reaction rate $\mu_a(n)$ of (2.7).[3] In actual computation, this solution is useful only for small N, otherwise one encounters a problem of convergence of the alternating series. Other methods of solving the master equation, such as calculating the eigenvalues of the evolution matrix or direct numerical solution, also become difficult when N is large.

The method we describe here is based on a large-N expansion for conditional averages. Therefore it is complementary to the series solution or direct numerical solution. The essential ideas have been described previously,[10] so we present only the main results here.

The quantity of interest is the conditional average

$$\chi(n_0, t) \equiv \langle f(n) \mid n_0 \rangle_t = \sum_{n=0}^{\infty} f(n)\, P(n, t \mid n_0) \tag{3.2}$$

where $f(n)$ is any function of the number of reactant molecules. The advantage of using the backward form of the master equation becomes apparent when (3.1) is combined with (3.2). One obtains immediately an equation for the conditional average,

$$\frac{d\chi(n_0, t)}{dt} = \mu(n_0)[\chi(n_0 - 1, t) - \chi(n_0, t)] \tag{3.3}$$

with $\chi(n_0,\ t=0) = f(n_0)$. We next consider only transition probabilities $\mu(n)$ that can be expressed in the form

$$\begin{aligned} \mu(n) &= F(N)\,\mu(n/N) \\ &= F(N)\,\tilde{\mu}(x) \end{aligned} \tag{3.4}$$

where $x = n/N$ is the reactant concentration and F any arbitrary function. The three foregoing models are all of this form, namely,

$$F_a(N) = \beta N, \qquad \tilde{\mu}_a(x) = x \exp[-(\theta_m - ax)^{-1}] \tag{3.5}$$

$$F_b(N) = \beta' N^2 \sqrt{T_0}, \quad \tilde{\mu}_b(x) = \frac{1}{2}\left(\frac{\theta_m}{\theta_0} - \frac{ax}{\theta_0}\right)^{1/2} x^2 \exp[-(\theta_m - ax)^{-1}] \tag{3.6}$$

$$F_c(N) = \beta'' N, \qquad \tilde{\mu}_c(x) = x(1-x) \tag{3.7}$$

where $a = (\theta_m - \theta_0)/x_0$, and β, β', β'' are constants which could be allowed to vary with N if necessary.

The significance of (3.4) is that the N dependence is now explicit and isolated. We next rewrite (3.3) as

$$\frac{\partial\tilde{\chi}(x_0, \tau)}{\partial\tau} = \tilde{\mu}(x_0)\, N\left[\tilde{\chi}\left(x_0 - \frac{1}{N}, \tau\right) - \tilde{\chi}(x_0, \tau)\right] \tag{3.8}$$

where $\tau = F(N)t/N$ and $\tilde{\chi}(x_0, \tau) = \chi(x_0, t)$ with $x_0 = n_0/N$. Henceforth we will suppress the tilde on χ and μ. By using a new time variable τ, we are now in a position to introduce the $1/N$ expansion. Notice that the factor $1/N$ appears in the definition of τ; this is because we want the lowest-order equation in the expansion of (3.8) to be in the same form as the macroscopic equation (2.3). Since this equation does not contain any effects of fluctuations, all the higher-order terms in the expansion represent corrections due to fluctuations.

Expanding $\chi(x_0 - 1/N, \tau)$ about the point x_0, we find that (3.8) becomes

$$\frac{\partial\chi(x_0, \tau)}{\partial\tau} + \mu(x_0)\frac{\partial\chi(x_0, \tau)}{\partial x_0} = \sum_{k=2}^{\infty} \frac{1}{N^{k-1}}(-1)^k \frac{\mu(x_0)}{k!}\frac{\partial^k\chi(x_0, \tau)}{\partial x_0^k} \tag{3.9}$$

This is still an exact equation so long as the transition rate μ can be decomposed according to (3.4). The form of (3.9) suggests that the right-hand side of the equation can be treated as a perturbation. We therefore look for a solution in the form

$$\chi(x_0, \tau) = \sum_{l=0}^{\infty} \frac{1}{N^l} \chi_l(x_0, \tau) \tag{3.10}$$

Inserting (3.10) into (3.9) and matching terms with the same power of $1/N$, we find that each function $\chi_l(x_0, \tau)$ obeys a first-order partial differential equation with an inhomogeneous term involving $\chi_k(x_0, \tau)$, $k \leqslant l-1$.[10] Specifically, one obtains

$$\chi_0(x_0, \tau) = f[\bar{x}(\tau)] \tag{3.11}$$

$$\chi_l(x_0, \tau) = -\int_{x_0}^{\bar{x}(\tau)} \frac{\mathscr{H}_\ell[y, \bar{x}(\tau)]}{\mu(y)}\, dy \tag{3.12}$$

where $\bar{x}(\tau)$ is the concentration determined by the macroscopic equation (2.3) with initial condition $\bar{x}(\tau = 0) = x_0$. In (3.12), H_l is a known function that involves χ_{l-1}, χ_{l-2},..., χ_0.[10] We see that the solution to the macroscopic equation plays a central role in the solution to the master equation. In fact, the time dependence of $\chi(x_0, \tau)$ appears only through the time dependence of $\bar{x}(\tau)$.

Further reduction of the first two $\chi_l(x_0, \tau)$ functions has been carried out in the case of pure death processes. The conditional average now becomes

$$\begin{aligned}\chi(x_0, \tau) = f(\bar{x}) &+ \frac{1}{N}[f^{(2)}(\bar{x})\chi_{1,2} + f^{(1)}(\bar{x})\chi_{1,1}] \\ &+ \frac{1}{N^2}[f^{(4)}(\bar{x})\chi_{2,4} + f^{(3)}(\bar{x})\chi_{2,3} + f^{(2)}(\bar{x})\chi_{2,2} + f^{(1)}(\bar{x})\chi_{2,1}] \\ &+ \cdots\end{aligned} \tag{3.13}$$

According to this result, the conditional average of an arbitrary function $f(x)$ can be calculated once the solution of the macroscopic equation is known. Explicit expressions of the $\chi_{l,k}[x_0, \bar{x}]$ in terms of $\bar{x}$ are given in the Appendix.

As (3.13) shows, the lowest-order solution for $\chi(x_0, \tau)$ is given simply by the function f evaluated at $\bar{x}(\tau)$, the solution to the macroscopic equations (2.3). It is clear that $\bar{x}(\tau)$ describes the time evolution of the

concentration in the absence of fluctuations, and this condition is obtained when $N \to \infty$. Taking the large-N limit of $\chi(x_0, \tau)$ gives

$$\lim_{N \to \infty} \langle f(x) | x_0 \rangle_\tau = f(\bar{x}) = \lim_{N \to \infty} \int f(x)\, h(x.\, \tau | x_0)\, dx \tag{3.14}$$

which implies

$$\lim_{N \to \infty} h(x, \tau | x_0) = \delta(x - \bar{x}) \tag{3.15}$$

with $h(x, \tau | x_0)$ being the probability distribution that is the analogue of $P(n, t | n_0)$ in continuous concentration space. Equation (3.13) shows that in an infinite system, the distribution is determined completely by the solution to the macroscopic equation and there are no fluctuations.

The natural quantity in any discussion of fluctuations is the variance. The mean squared deviation in the property $f(x)$ can be formulated in a manner analogous to (3.2). One finds

$$\langle f^2(x) | x_0 \rangle - [\langle f(x) | x_0 \rangle]^2 = \frac{2}{N} \chi_{1,2}(x_0, \tau)\, f'^2(\bar{x}) + O\left(\frac{1}{N^2}\right) \tag{3.16}$$

For $f(x) = x$, the quantity

$$\sigma_{sc}^2(\tau) \equiv 2\chi_{1,2}(x_0, \tau) = \lim_{N \to \infty} N[\langle x^2 | x_0 \rangle_\tau - \langle x | x_0 \rangle_\tau^2] \tag{3.17}$$

will be called the scaled variance in the concentration. The procedure of expressing the moments in a $1/N$ series can be applied to any order. One can consider two types of moments: one is the deviation from the macroscopic description $\bar{x}(\tau)$, and the other is the deviation from the actual average concentration $\langle x | x_0 \rangle_\tau$. The different moments are, of course, related through the expression

$$\langle x | x_0 \rangle_\tau = \bar{x}(\tau) + \frac{1}{N} \chi_{1,1}(x_0, \tau) + \frac{1}{N^2} \chi_{2,1}(x_0, \tau) + \cdots \tag{3.18}$$

In order to compare the distribution function with a Gaussian, the following moments are useful:

$$M_2(\tau) = \frac{2}{N} \chi_{1,2} + \frac{2}{N^2} \left[\chi_{2,2} - \frac{1}{2} \chi_{1,1}^2 \right] + O\left(\frac{1}{N^3}\right) \tag{3.19}$$

$$M_3(\tau) = \frac{6}{N^2}\left[\chi_{2,3} - \chi_{1,1}\chi_{1,2}\right] + O\left(\frac{1}{N^3}\right) \tag{3.20}$$

$$M_4(\tau) = \frac{24}{N^2}\chi_{2,4} + \frac{24}{N^3}\left[\chi_{3,4} - \chi_{1,1}\chi_{2,3} + \frac{1}{2}\chi_{1,1}^2\chi_{1,2}\right] \tag{3.21}$$

where the moments $M_k(\tau)$ are defined by

$$M_k(\tau) = \langle (x - \langle x \mid x_0 \rangle_\tau)^k \mid x_0 \rangle_\tau \tag{3.22}$$

Explicit expressions for the $\chi_{k,l}$ can be found in the Appendix. It should be noted that the foregoing results are restricted to the class of models involving only pure death processes and with $\mu(n)$ separable in the sense of (3.4), otherwise they are completely general.

Although an extensive study of the differences between the $1/N$ expansion[10] described here and the Ω expansion of Van Kampen[8] can be found in ref. 10, we briefly recall the basic ideas to facilitate the understanding of this section.

The master equation description of a stochastic process has two equivalent forms, namely a backward and a forward form . The forward form of the master equation was used by Van Kampen as a starting point for his size or Ω expansion.[8] It describes the time evolution of the probability function, which then gives rise to conditional averages. Van Kampen's method has the disadvantage that higher approximations of the distribution function are difficult to find.

The backward form of the master equation, still an equation for the distribution function and completely equivalent to the forward form, can be averaged directly to yield an equation for conditional averages. This equation was the starting point for the size expansion of arbitrary conditional averages proposed in ref. 10. No difficulties arise when extending the approximations to successive higher orders. By expanding an arbitrary conditional average in powers of $1/N$, it is possible to find also the distribution function itself. In the limit of large Ω, a Gaussian distribution arises, which is in agreement with the so-called linear noise approximation.

4. MOLECULAR DYNAMICS SIMULATION

In this section we describe the simulation model for the molecular dynamics part of our study and the procedures used to generate the results that will be compared to those derived from the macroscopic equation (Section 2) and from the $1/N$ expansion (Section 3). To model adiabatic explosion under bimolecular reactions, we consider a binary mixture of

two-dimensional hard disks which are identical except that species A, being the reactant particles, can undergo reactive collisions of the type described by (2.2), whereas species B, being the product particles, cannot. The condition for a reactive collision is $T_{\text{rel}} > U$, where T_{rel} is the relative kinetic energy of the colliding particles along the centerline of the pair at contact. We have previously demonstrated that this model of reaction kinetics leads to an Arrhenius temperature dependence consistent with the assumption made in Section 2.[11] For A–A collisions which do not satisfy the condition $T_{\text{rel}} > U$, the dynamics is treated correctly for the elastic scattering of hard disks; for all A–B and B–B collisions regardless of T_{rel}, only elastic scattering is allowed.

A particular simulation run begins with all the particles being of species A and continues until most are converted to species B. The concentration of species A and the system temperature, defined in terms of the total kinetic energy of the particles, are monitored as the simulation proceeds. During simulation the system is periodic along one direction, while along the other direction the boundaries are rigid walls where any arriving particle will be specularly reflected.

It is clear from the foregoing description that the simulation model is constructed to correspond to reaction model b. As we have shown in Section 2, this model is specified by three parameters, θ_m, θ_0, and the initial concentration x_0. Once their values are chosen and the number of particles N is fixed, the simulation will give the temporal variation of the concentration of species A and the temperature.

We have investigated two system sizes, $N = 50$ and 800, for a relatively high-temperature condition, $\theta_m = 0.6$ and $\theta_0 = 0.2$. In each case 100 independent runs (with different random number sequences) are made and the results averaged to given $\langle x \rangle$, $N[\langle x^2 \rangle - \langle x \rangle^2]$, and $NP(x)$.

5. NUMERICAL RESULTS

We will present four types of results using the three adiabatic explosion models described in Section 2 and two sets of temperature parameters. The four types of results are the solutions to the macroscopic equation (2.3) by numerical integration, the solutions to the master equation (2.6) with reaction rate $\mu_b(n)$ by numerical integration, the moments (3.18)–(3.21) obtained by the method of $1/N$ expansion, and MD results from Section 4. The temperature sets are $\theta_0 = 0.2$, $\theta_m = 0.6$ (hot condition) and $\theta_0 = 0.08$, $\theta_m = 0.2$ (cold condition). Much of the calculations presented will be for explosion model b, although we will also discuss corresponding results for models a and c.

Our interest in the solutions to (2.3) is twofold. First it provides the

macroscopic description of a given model, the solution $\bar{x}$ being entirely determined by the death rate $\mu(x)$. By comparing $\bar{x}$ and $\mu(x)$ for different models one can see quite simply the basic characteristics of each model. Secondly, since (2.3) contains no information about the higher-order moments, its solution becomes the natural reference for the delineation of fluctuation effects.

Figure 1 shows a comparison of the death rate $\mu(x)$ for models *a* and *b* at the hot and cold conditions, along with model *c*, which is temperature independent. The unimolecular reaction rate (model *a*) is seen to be somewhat larger than the binary collision model (model *b*); as can be expected, both rates are greater, the higher the temperature. The corresponding time-dependent average concentrations given by (2.3) are shown in Fig. 2. In obtaining these results, we first determine the concentration $\bar{x}_c$ at the inflection point where $d^2\bar{x}/dt^2 = 0$. Then the characteristic time τ_c defined by the integral

$$\tau_c = \int_{\bar{x}_0}^{\bar{x}_c} \frac{dx}{\mu(x)} \tag{5.1}$$

where $\bar{x}_0$ is the initial concentration, can be computed by quadrature. Physically, τ_c is the time at which the macroscopic concentration shows an inflection point. For the two temperature conditions the values of τ_c differ widely, 48.9 and 40,007 for the hot and cold conditions, respectively. The data showing the variation of $\bar{x}$ with τ in Fig. 2 are obtained by choosing a sequence of $\bar{x}$ values and determining the corresponding τ by using (5.1) with $\bar{x}_c$ replaced by $\bar{x}$.

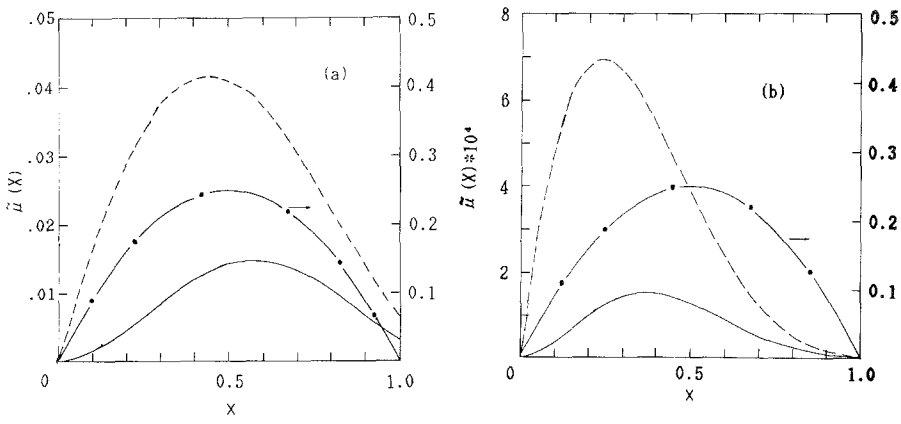

Fig. 1. Concentration dependence of reaction-rate models *a* (dashed curve), *b* (solid curve), and *c* (dotted curve) for (a) hot condition and (b) cold condition.

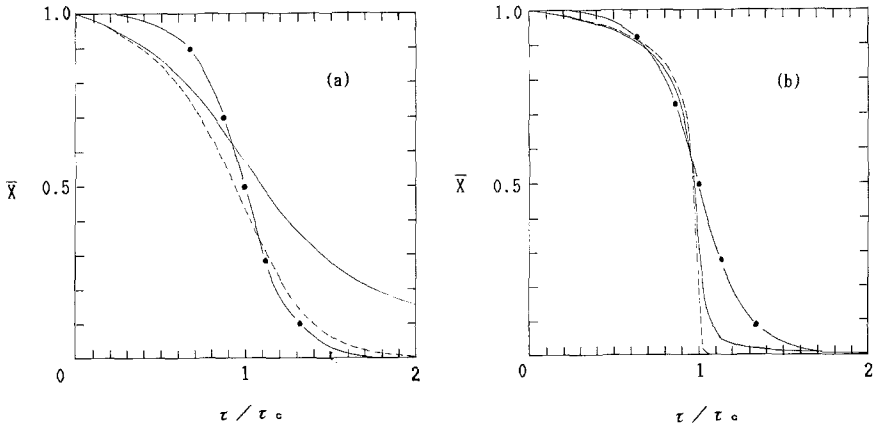

Fig. 2. Variation of the macroscopic concentration with time for the reaction-rate models *a* (dashed curve), *b* (solid curve), and *c* (dotted curve); the dimensionless time τ is in units of the correlation time τ_c. (a) Hot condition, $\tau_c = 48.9$, and (b) cold condition, $\tau_c = 40{,}007$.

Keeping in mind that the time scales for the hot and cold temperature conditions differ by three orders of magnitude, one sees in Fig. 2 that both models *a* and *b* show a more pronounced "critical behavior" at the cold condition. On the basis of Figs. 1 and 2, one may expect that models *a* and *b* are not very different qualitatively. Since we are interested in comparing the master equation solutions with molecular dynamics (MD) data, we will mostly consider model *b* in the following discussions.

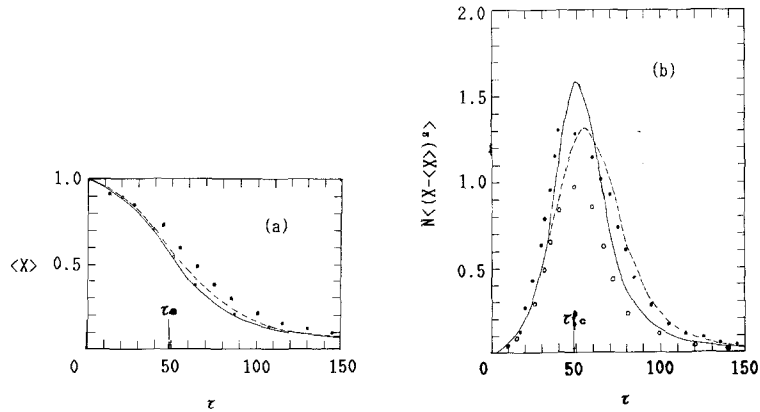

Fig. 3. Comparison of (a) average concentration $\langle x \rangle$ and (b) variance $N\langle (x - \langle x \rangle)^2 \rangle$ for reaction-rate model *b* and the hot condition; results for $N = 50$ are denoted by the dashed curves (master equation) and closed circles (MD), whereas for $N = 800$ they are labeled by solid curves (master equation) and open circles (MD).

For the master equation (2.6) we have obtained two types of solutions, a direct numerical solution for a series of N values and correpondingly solutions for the first four fluctuation moments M_k as developed in Section 3. First we consider a comparison of master equation and MD results for the same N. Figure 3 shows the average concentration and the variance for two N values, $N=50$ and $N=800$. While the two methods of calculation give qualitatively similar results, we see that MD data show more statistical variations, no doubt due mostly to the small number of particles in the system. Moreover, the fact that there is substantial agreement between the solutions at the larger N indicates that these two very different descriptions have already converged at the level of $\langle x \rangle$ and $\langle x^2 \rangle$ for a system of 1000 particles. Notice that the comparison with MD is carried out for the hot condition only; the large value of τ_c for the cold condition makes it unfeasible to carry out simulation on such a time scale.

Although we have solved the master equation by direct integration for a series of N values, the computational efforts involved when N is large are considerable. Thus, it would be very desirable to know the N values for which we can apply the $1/N$ expansion. First we show how the concentration moments $\langle x^n \rangle$ vary with N. Results for the first four moments are shown in Figs. 4–7; in each case both hot and cold conditions are considered. In the case of Fig. 4 we show the average concentration as deviations from the

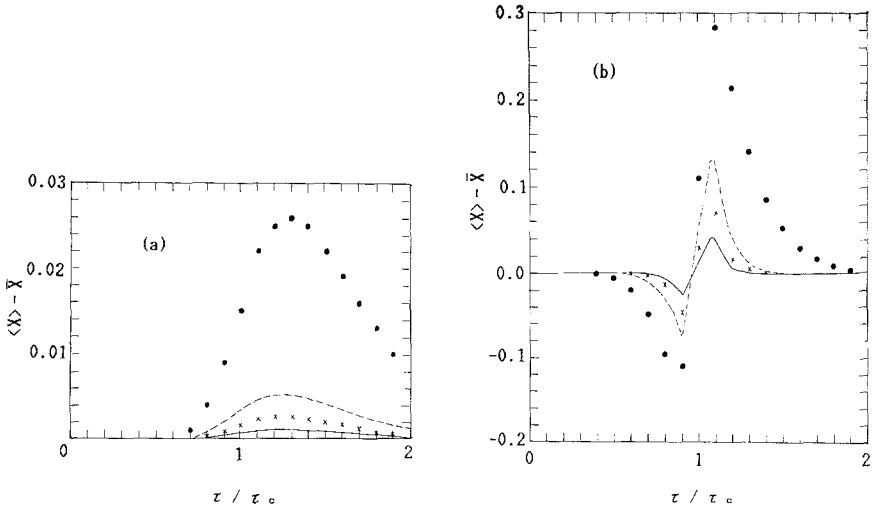

Fig. 4. Deviation of concentration $\langle x \rangle$ given by the master equation from the solution $\bar{x}$ to the macroscopic equation for $N=100$ (closed circles), 500 (dashed curves), 1000 (crosses), and 2000 (solid curves), for (a) hot condition and (b) cold condition. Dimensionless time τ is in units of the correlation time τ_c.

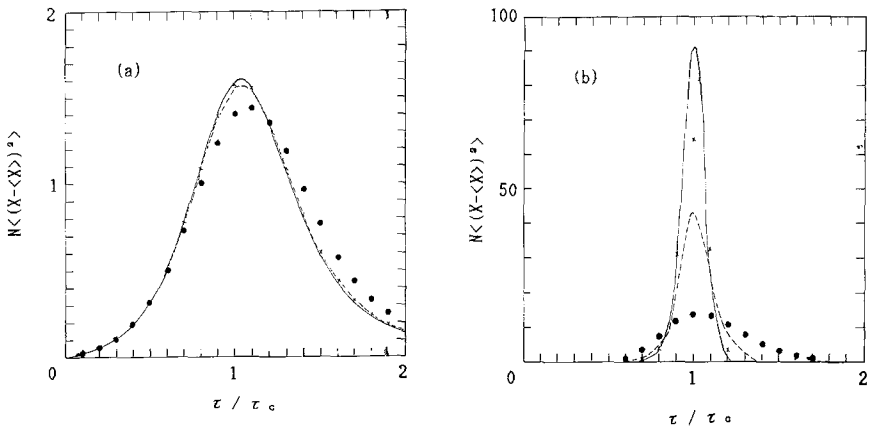

Fig. 5. Same as Fig. 4, for the concentration variance $N\langle(x-\langle x\rangle)^2\rangle$.

macroscopic solution, the limiting behavior for large N. One sees a significant change from $N=100$ to $N=500$, and smaller deviations with further increases in N. Using these results, one can determine the value of N needed to reach a certain degree of convergence. The other moments show similar behavior. For a pure Gaussian distribution the moments of Figs. 6 and 7 should vanish. It is interesting to note that the deviations from the macroscopic concentration show different time variations for the two temperature conditions; there are positive deviations for the hot condition, whereas for the cold condition the deviations change sharply in sign around τ_c. According to (3.18) for large N the deviation from the macro-

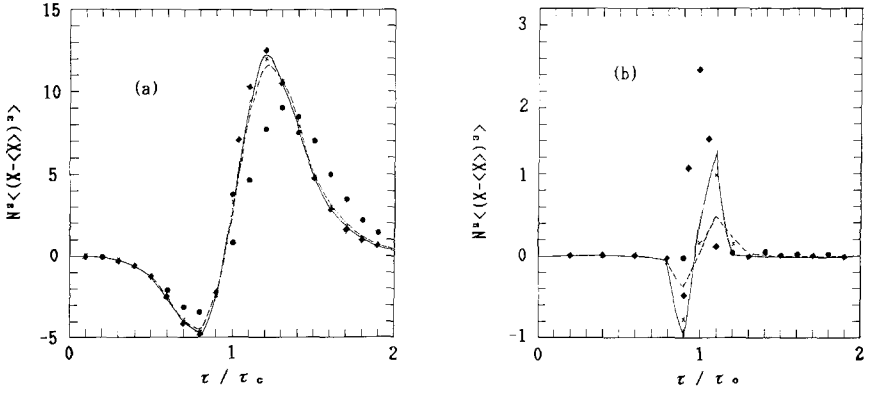

Fig. 6. Same as Fig. 4, for the third-order moment $N^2\langle(x-\langle x\rangle)^3\rangle$. Limiting results of the $1/N$ expansion are shown as diamonds.

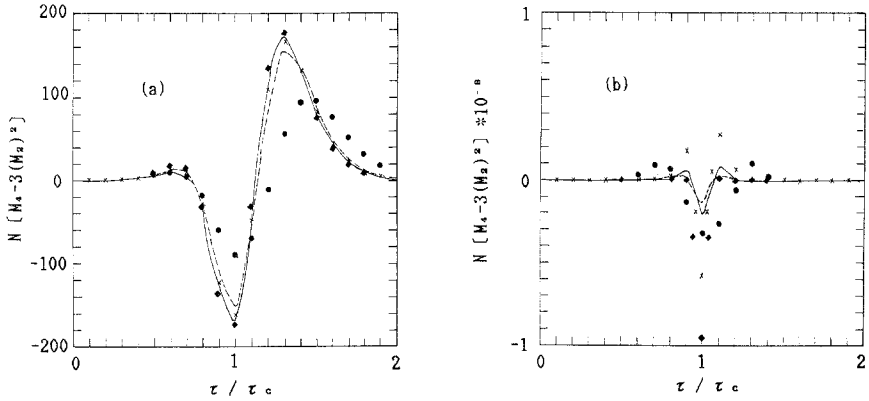

Fig. 7. Same as Fig. 6, for $N^2[M_4 - 3(M_2)^2]$, except that in case (b) different results have different scales as indicated; results are shown for $N = 100$, times 10^3 (closed circles); for $N = 500$ and 1000, times 10 (dashed curves and crosses, respectively); for $N = 2000$ (solid curves); and for the limit of the $1/N$ expansion, times 10^{-1} (diamonds).

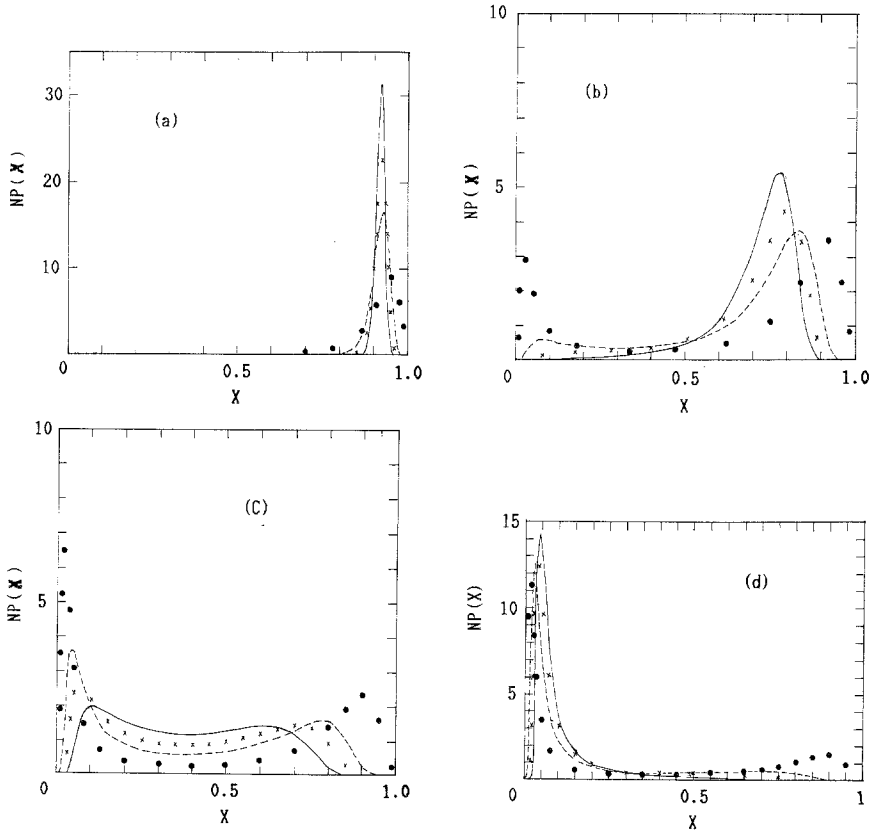

Fig. 8. Time evolution of probability distribution of concentration as given by the master equation for model b and cold condition for $N = 100$ (closed circles), 500 (dashed curves), 1000 (crosses), and 2000 (solid curves); results are shown at times $\tau/\tau_c =$ (a) 0.6, (b) 0.9, (c) 1.0, (d) 1.1.

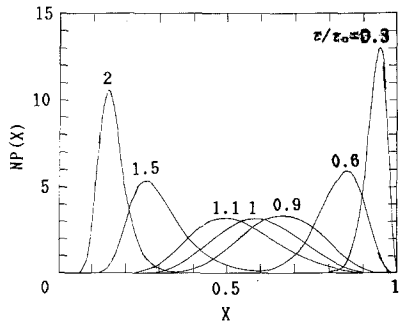

Fig. 9. Same as Fig. 8, except that only the $N = 100$ results are shown at various τ/τ_c and the temperature condition is the hot condition.

scopic equation is determined by $\chi_{1,1}$ [see (A10)], which is given in terms of $\mu(\bar{x})$ and its derivative $\mu^{(1)}(\bar{x})$.

The comparison between direct numerical solutions and the $1/N$ expansion is shown in Tables I–IV. The validity of the expansion is seen to be quite sensitive to the temperature condition, and the behavior is

Table I. Percent Deviation of Average Concentration $\langle x|x_0\rangle_\tau$ Obtained by Using the *N* Expansion from That Derived Numerically from the Master Equation, Hot Sample Condition ($\theta_0 = 0.2$, $\theta_m = 0.6$)

τ/τ_c	$N = 100$	$N = 500$	$N = 1000$	$N = 2000$
0.1	0.00	0.00	0.00	0.00
0.2	0.00	0.00	0.00	0.00
0.3	0.01	0.01	0.01	0.01
0.4	0.00	0.00	0.00	0.00
0.5	0.00	0.00	0.00	0.00
0.6	−0.02	0.00	0.00	0.00
0.7	−0.06	0.00	0.00	0.00
0.8	−0.08	0.00	0.00	0.00
0.9	−0.06	0.00	0.00	0.00
1.0	0.07	0.00	0.00	0.00
1.1	0.20	0.00	0.00	0.00
1.2	0.21	0.00	0.00	0.00
1.3	0.17	0.00	0.00	0.00
1.4	0.16	0.00	−0.01	0.00
1.5	0.22	−0.01	0.00	0.00
1.6	0.28	−0.02	−0.02	−0.03
1.7	0.33	−0.02	−0.03	−0.03
1.8	0.34	−0.03	−0.05	−0.05
1.9	0.33	−0.04	−0.05	−0.06
2.0	0.29	−0.07	−0.08	−0.08

Table II. Percent Deviation of Average Concentration $\langle x|x_0\rangle_\tau$ Obtained by Using the N Expansion from That Derived Numerically from the Master Equation, Cold Sample Condition ($\theta_0=0.08$, $\theta_m=0.2$)

τ/τ_c	$N=100$	$N=500$	$N=1000$	$N=2000$
0.1	0.00	0.00	0.00	0.00
0.2	0.02	0.02	0.02	0.02
0.3	0.02	0.01	0.03	0.01
0.4	0.01	0.01	0.01	0.01
0.5	−0.05	0.01	0.01	0.01
0.6	−0.29	0.00	0.00	0.00
0.7	1.0	−0.03	0.00	0.00
0.8	28	−0.01	−0.04	0.00
0.9	499	19	3.7	0.54
1.0	−4480	−211	−55	−14
1.1	−2076	−129	−31	−3.6
1.2	−90	24	12	1.9
1.3	45	22	3.3	0.36
1.4	68	8.3	0.68	0.07
1.5	72	2.5	0.21	0.00
1.6	72	0.94	0.09	−0.02
1.7	68	0.53	0.03	−0.06
1.8	62	0.54	0.11	0.02
1.9	55	0.32	−0.09	−0.18
2.0	49	0.55	0.08	−0.03

different for the two temperature conditions. For the hot condition the $1/N$ expansion works well except possibly in the smallest system examined ($N=100$). Since the N expansion gives the correct short-time limit [with $\chi_{1,1}$ and $\chi_{2,1}$ vanishing in (3.18)], the deviations at very short times (cf. Table III) are believed to arise from numerical inaccuracies which are made worse by showing the results as a percentage. The absolute deviations are actually quite small; for example, at $\tau/\tau_c=0.1$ (Table III) they are around 0.0016. For the cold condition the $1/N$ expansion breaks down quite badly in the immediate vicinity of τ_c; at $N=2000$ there is still a sizeable discrepancy in the second moment (Table IV).

The behavior of the probability distribution $P(x, \tau|\tau_0)$, as obtained by direct numerical solution of (2.6) for model b, is shown in Figs. 8 and 9 for the cold and not conditions, respectively. In the former we include the results for all four N values, whereas in the latter we show only the results for the smallest system, $N=100$. In Fig. 8 we see a clear display of bimodal concentration distribution in the immediate vicinity of $\tau=\tau_c$, the effect being more pronounced, the smaller the system size. By contrast, in Fig. 9 the concentration distribution at $N=100$ shows only a single peak at all

Table III. Percent Deviation of Second Moment $M_2(\tau)$ Obtained by Using the N Expansion from That Derived Numerically from the Master Equation, Hot Sample Condition ($\theta_0 = 0.2$, $\theta_m = 0.6$)

τ/τ_c	$N = 100$	$N = 500$	$N = 1000$	$N = 2000$
0.1	−0.09	−0.08	−0.08	−0.08
0.2	−0.21	−0.15	−0.15	−0.15
0.3	−0.33	−0.17	−0.16	−0.15
0.4	−0.47	−0.11	−0.10	−0.10
0.5	−0.68	−0.08	−0.06	−0.05
0.6	−0.63	−0.06	−0.03	−0.02
0.7	0.36	−0.01	−0.02	−0.02
0.8	2.7	2.4	0.02	0.00
0.9	4.7	0.22	0.06	0.01
1.0	3.7	0.14	0.04	0.01
1.1	−1.8	−0.15	−0.04	−0.01
1.2	−6.6	−0.38	−0.11	−0.04
1.3	−7.5	−0.36	−0.10	−0.05
1.4	−4.8	−0.17	−0.06	−0.04
1.5	−0.71	0.09	−0.02	−0.01
1.6	3.0	0.20	0.00	−0.05
1.7	5.6	0.26	0.00	−0.07
1.8	7.2	0.25	−0.02	−0.09
1.9	7.4	0.32	−0.05	−0.12
2.0	7.0	0.11	−0.12	−0.17

times, and we can be sure that the distribution will remain unimodal in the large-N systems. Thus, the bidurcation behavior is dependent on system size and the temperature condition.

6. DISCUSSIONS

In this work we have investigated the effects of fluctuations in the particularly simple case of exothermic reaction in a closed system with nonlinearities arising from the Arrhenius kinetics and from collisions (model *b*). Results from three consistent levels of descriptions are presented. The temporal behavior of the reactant concentration, determined by numerically integrating the macroscopic rate equation, plays the role of reference results in which fluctuation effects are totally absent. Fluctuation effects are delineated mainly through the master equation description, in terms of direct numerical integrations for several system sizes N, and by a $1/N$ expansion of the variance and higher-order deviations from the average concentration. In addition, some molecular dynamics results are presented

Table IV. Percent Deviation of Second Moment $M_2(\tau)$ Obtained by Using the N Expansion from That Derived Numerically from the Master Equation, Cold Sample Condition ($\theta_0 = 0.08$, $\theta_m = 0.2$)

τ/τ_c	$N=100$	$N=500$	$N=1000$	$N=2000$
0.1	−0.13	−0.24	−0.25	−0.25
0.2	−0.69	−1.3	−1.3	−1.3
0.3	1.8	−0.58	−0.64	−0.65
0.4	10	−0.11	−0.32	−0.37
0.5	33	0.53	−0.22	−0.39
0.6	53	4.0	0.82	0.13
0.7	44	19	4.4	0.93
0.8	−64	34	21	6.3
0.9	−1890	−121	−26	2.1
1.0	76223	4628	1437	451
1.1	−1266	−41	24	42
1.2	69	91	86	59
1.3	96	95	74	19
1.4	99	91	32	5.0
1.5	99	73	8.8	1.7
1.6	99	34	3.1	0.59
1.7	99	10	1.3	0.17
1.8	99	3.9	0.74	0.16
1.9	99	1.8	0.17	−0.18
2.0	98	1.4	0.28	−0.00

to show how the rate equation and the master equation can be modeled by a system of particles undergoing collision-induced reactions.

We have shown that the two parameters, initial and maximum temperatures θ_0 and θ_m, strongly influence both the macroscopic and the fluctuation behavior of the model. At the high-temperature condition the reaction rate is two orders of magnitude larger, the incubation time τ_c (time at which the reactant concentration goes through an inflection point) is much shorter, and as a result the temporal variation of the macroscopic reactant concentration is relatively more gradual (cf. Figs. 1 and 2). Correspondingly, one finds that fluctuations slow down the reactant consumption (Fig. 4a). In contrast, at the low-temperature condition, τ_c is greater by three orders of magnitude and the decrease of macroscopic reactant concentration is much sharper at the inflection point. An asymmetry now appears in the deviation from macroscopic solution in that fluctuations cause an increase in reactant prior to τ_c and a decrease in consumption after τ_c (Fig. 4b).

From a comparison of the macroscopic solutions for the two

temperature conditions (Fig. 2) we can anticipate that fluctuations will play a more pronounced role at the cold condition. It is then not too surprising that the system exhibits transient bimodality, a characteristic of strong, nonlinear fluctuations, at the cold condition. This behavior is not observed at the hot condition. In this connection we should remark that master equation results for reaction model *c* (which we have not shown explicitly) do not show bimodality behavior. Since the model does not consider Arrhenius kinetics and is therefore temperature independent, this is consistent with our conclusion that biomodality is associated with both strong nonlinearities and fluctuations, the latter being most enhanced in small systems. In the limit of large N, bimodality should not appear, as all fluctuation effects vanish.

Because of the very different time scales involved between the two temperature conditions examined here, we are able to apply molecular dynamics simulation only in the high-temperature condition. A direct comparison of particle simulation results and master equation calculations at the same values of N (Fig. 3) leads to the following conclusions. For small N ($N = 50$) there is some discrepancy between these two approaches, probably due to statistical fluctuations in the simulation data, which are based on 100 independent runs for each value. The agreement at large N ($N = 800$) is quite pleasing, thus confirming the equivalence of our formulations of the two descriptions and the fact that the $1/N$ expansion discussed in Section 3 will be useful for examining the behavior of even larger systems.

In closing, we note that the particle simulation approach to studies of chemically reactive systems can play a unique role in elucidating the importance of molecular-scale effects and testing theoretical assumptions concerning local equilibrium and spatial homogeneities. Recently it has been shown that deviations from Maxwellian valocity distribution caused by reactive collisions can give rise to a correction to the reaction rate.[12] In the understanding of chemical oscillations, the question of spontaneous symmetry breaking in connection with the onset of "critical" or instability behavior is an issue which simulation can help address.[13] In view of the continuing increase of computing power and interest in simulation and modeling, further studies clarifying the nature and importance of nonequilibrium or inhomogeneous effects can be highly worthwhile.

APPENDIX

According to Eq. (3.12), the functions $\chi_l(x_0, \tau)$ are known once the functions H_l are given. Previously we have presented explicit expressions for H_l,[10] namely,

$$H_l[x_0, \bar{x}] = \sum_{s=2}^{l+1} \frac{(-1)^s \mu(x_0)}{s!} \frac{d^s}{dx_0^s} \chi_{l+1-s}[x_0, \bar{x}] \tag{A1}$$

with

$$\chi_0[x_0, \bar{x}] = f(\bar{x}) \tag{A2}$$

The derivatives of (A1) can be carried out explicitly using the relation[10,14]

$$\frac{d\bar{x}}{dx_0} = \frac{\mu(\bar{x})}{\mu(x_0)} \tag{A3}$$

For calculating the moments up to M_4 we need H_1, H_2, and H_3 explicitly. The manipulations involved are quite lengthy, so we will illustrate the procedure by restricting ourselves to H_1:

$$H_1 = \frac{\mu(x_0)}{2!} \frac{d^2 f(\bar{x})}{dx_0^2} \tag{A4}$$

Using (A3), we can express the derivatives of $f(\bar{x})$ in terms of $\mu(x_0)$, $\mu(\bar{x})$, and the derivatives of f with respect to its argument, denoted by $f^{(n)}$. We get

$$\begin{aligned} \frac{df(\bar{x})}{dx_0} &= f^{(1)}(\bar{x}) \frac{d\bar{x}}{dx_0} \\ &= \frac{\mu(\bar{x})}{\mu(x_0)} f^{(1)}(\bar{x}) \end{aligned} \tag{A5}$$

and

$$\frac{d^2 f(\bar{x})}{dx_0^2} = f^{(2)}(\bar{x}) \left[\frac{\mu(\bar{x})}{\mu(x_0)}\right]^2 + f^{(1)}(\bar{x}) \frac{\mu(\bar{x})[\mu^{(1)}(\bar{x}) - \mu^{(1)}(x_0)]}{\mu^2(x_0)} \tag{A6}$$

Inserting (A6) into (3.12), one finds for the function χ_1 the expression

$$\chi_1(x_0, \bar{x}) = f^{(2)}(\bar{x}) \chi_{1,2} + f^{(1)}(\bar{x}) \chi_{1,1} \tag{A7}$$

with

$$\chi_{1,2} = \frac{1}{2} \mu^2(\bar{x}) \int_{\bar{x}}^{x_0} \frac{1}{\mu^2(y)} dy \tag{A8}$$

and

$$\chi_{1,1} = \frac{\mu(\bar{x})}{2} \int_{\bar{x}}^{x_0} \frac{\mu^{(1)}(\bar{x}) - \mu^{(1)}(y)}{\mu^2(y)} dy \tag{A9}$$

After integration by parts, (A9) can be simplified further to give

$$\chi_{1,1}=\frac{\mu^{(1)}(\bar{x})}{\mu(\bar{x})}\chi_{1,2}+\frac{\mu(\bar{x})}{2\mu(x_0)}-\frac{1}{2} \tag{A10}$$

For the remaining functions $\chi_{l,k}$ we only give the results:

$$\chi_{2,4}(x_0,\tau)=\frac{1}{2}(A_2)^2 \tag{A11}$$

$$\chi_{2,3}(x_0,\tau)=\chi_{1,1}\chi_{1,2}+\frac{2\mu'(\bar{x})}{\mu(\bar{x})}(A_2)^2+2A_3-A_2 \tag{A12}$$

$$\begin{aligned}\chi_{2,2}(x_0,\tau)=&\frac{1}{2}(\chi_{1,1})^2+\left[\frac{3\mu'^2(\bar{x})}{\mu^2(\bar{x})}+\frac{2\mu''(\bar{x})}{\mu(\bar{x})}\right](A_2)^2\\&+\left[\frac{\mu'(\bar{x})}{\mu(x_0)}-\frac{5}{2}\frac{\mu'(\bar{x})}{\mu(\bar{x})}\right]A_2\\&+\frac{6\mu'(\bar{x})}{\mu(\bar{x})}A_3+\frac{1}{4}\frac{\mu^2(\bar{x})}{\mu^2(x_0)}-\frac{1}{4}\frac{\mu(\bar{x})}{\mu(x_0)}\end{aligned} \tag{A13}$$

$$\begin{aligned}\chi_{2,1}(x_0,\tau)=&\frac{1}{2}\frac{\mu'(\bar{x})}{\mu(\bar{x})}\chi_{1,1}^2+\frac{\mu''(\bar{x})}{\mu(\bar{x})}\chi_{1,2}\chi_{1,1}+\left[\frac{\mu'(\bar{x})\,\mu''(\bar{x})}{\mu^2(\bar{x})}+\frac{1}{2}\frac{\mu'''(\bar{x})}{s(\bar{x})}\right](A_2)^2\\&+\left[\frac{\mu'^2(\bar{x})}{\mu^2(\bar{x})}+\frac{\mu''(\bar{x})}{\mu(\bar{x})}\right]A_3-\frac{1}{2}\frac{\mu''(\bar{x})}{\mu(\bar{x})}A_2\\&+\frac{1}{12}\frac{\mu(\bar{x})\,\mu'(x_0)}{\mu^2(x_0)}-\frac{1}{12}\frac{\mu'(\bar{x})}{\mu(\bar{x})}\end{aligned} \tag{A14}$$

$$\begin{aligned}\chi_{3,4}=&\chi_{2,2}\chi_{1,2}+\chi_{1,1}[\chi_{2,3}-\chi_{1,2}\chi_{1,1}]+(A_2)^3\left[\frac{4}{3}\frac{\mu''(\bar{x})}{\mu(\bar{x})}+\frac{16}{3}\frac{\mu'^2(\bar{x})}{\mu^2(\bar{x})}\right]\\&+12\frac{\mu'(\bar{x})}{\mu(\bar{x})}A_2A_3-5\frac{\mu'(\bar{x})}{\mu(\bar{x})}(A_2)^2+6A_4-3A_3+\frac{7}{12}A_2\end{aligned} \tag{A15}$$

For arbitrary death rates the functions $A_l(x_0,\bar{x})$, defined by

$$A_l=\frac{\mu^l(\bar{x})}{l!}\int_{\bar{x}}^{x_0}\mu^{-l}(y)\,dy \tag{A16}$$

can only be calculated numerically.

ACKNOWLEDGMENT

S. Yip acknowledges support by the National Science Foundation during the course of this work.

REFERENCES

1. G. Nicolis and I. Prigogine, *Self-Organization in Nonequilibrium Systems* (Wiley, New York, 1977); G. Nicolis, G. Dewel, and J. W. Turner, eds., *Order and Fluctuations in Equilibrium and Nonequilibrium Statistical Mechanics* (Wiley, New York, 1981); L. Arnold and R. Lefever, eds., *Stochastic Nonlinear Systems* (Springer, Berlin, 1980).
2. G. Nicolis, F. Baras, and M. Malek Mansour, in *Nonlinear Phenomena in Chemical Dynamics*, A. Pacault and C. Vidal, eds. (Springer-Verlag, Berlin, 1981), p. 104.
3. F. Baras, G. Nicolis, M. Malek Mansour, and J. W. Turner, *J. Stat. Phys.* **32**:1 (1983).
4. G. Nicolis and F. Baras, *J. Stat. Phys.* **48**:1071 (1987).
5. N. V. Kondratiev and E. Nikitin, *Gas-Phase Reactions* (Springer-Verlag, Berlin, 1981).
6. G. H. Weiss, *J. Stat. Phys.* **6**:179 (1972).
7. I. Oppenheim, K. E. Shuler, and G. H. Weiss, *Stochastic Processes in Chemical Physics* (MIT Press, Cambridge, Massachusetts, 1977).
8. N. G. van Kampen, *Stochastic Processes in Physics and Chemistry* (North-Holland, Amsterdam, 1981).
9. P. Hänggi and H. Thomas, *Phys. Rep.* **88**:207 (1982).
10. O. J. Eder and T. Lackner, *Phys. Rev. A* **28**:952 (1983); O. J. Eder, T. Lackner, and M. Posch, *Phys. Rev. A* **31**:366 (1985).
11. D.-P. Chou, Ph.D. Thesis, MIT, Cambridge, Massachusetts (1981); D.-P. Chou and S. Yip, *Combust. Flame* **58**:239 (1984).
12. F. Baras and M. Malek Mansour, *Phys. Rev. Lett.* **63**:2429 (1989); see also F. Baras and G. Nicolis, in *Microscopic Simulations of Complex Flows*, M. Mareschal, ed. (Plenum Press, New York, 1990), p. 339.
13. G. Nicolis, A. Amellal, G. Dupont, and M. Mareschal, *J. Mol. Liq.* **41**:5 (1989); F. Baras, J. Pearson, and M. Malek Mansour, *J. Chem. Phys.* **93**:5747 (1990); see also M. Mareschal, in *Microscopic Simulations of Complex Flows*, M. Mareschal, ed. (Plenum Press, New York, 1990), p. 141.
14. T. Lackner and S. Yip, *Phys. Rev. A* **31**:451 (1985).